SPECTROSCOPIC MEASUREMENT AND NUMERICAL ANALYSIS OF MEDIUM-POWER HYDROGEN/NITROGEN-MIXTURE ARCJET FLOWFIELDS

H. Tahara*, T. Yonezawa**, Y. Andoh**, K. Onoe+ and T. Yoshikawa+

Faculty of Engineering Science, Osaka University

Toyonaka, Osaka, Japan

Abstract

Spectroscopic measurement was carried out to understand the plasma features in a 10-kW-class water-cooled direct-current arcjet. Ammonia and a mixture of nitrogen and hydrogen were used as propellants. In the mixture of N_2+nH_2, the H_2 mole fraction n was varied from 0.5 to 3.0, in which a H_2 mole fraction of 3.0 corresponded to that of ammonia. The discharge voltage and the vacuum tank pressure for N_2+3H_2 were higher than those for NH_3 at a constant discharge current and a constant input power, respectively, because of the difference of particles species generated in their arc discharges. These characteristics agreed with those of H-atom electronic excitation temperatures and electron number densities in the constrictor. The NH_3 and N_2+3H_2 plasmas in the constrictor were expected to be nearly in a temperature-equilibrium condition. On the other hand, the plasmas in the expansion nozzle were in thermodynamical nonequilibrium, because the electron number densities drastically decreased downstream. As a result, the H-atom excitation temperature and the N_2 rotational excitation temperature decreased from 7000-11000 K in the constrictor to about 4000 K and to 1000-1500 K, respectively, on the nozzle exit at input powers of 7-12 kW, although the NH rotational excitation temperature did not axially decrease significantly because of its longer relaxation time of rotational excitation.

Introduction

The 10-kW-class direct-current arcjet thruster is a promising device suitable for future missions for planetary exploration and construction of large stations. The recent research and development of arcjet thrusters encounter significant problems as follows: (1) low thrust efficiency; (2) severe electrode erosion. These features are related to arc structure and flowfield in arcjet chambers. However, inner plasma properties are not clear because of the complicated flowfield including the interaction between arc and gas flow, energy transfer and internal energy excitations of atoms and molecules etc.

In a previous study, we examined nitrogen plasma properties in an arcjet discharge chamber by means of optical diagnostics in order to understand the arc structure and the thermodynamical nonequilibrium flowfield.[1-7] Electron densities and several temperatures such as atomic electronic excitation and molecular vibrational and rotational excitation temperatures were evaluated. However, ammonia and a mixture of nitrogen and hydrogen are used familiarly as propellants. Their plasmal properties are unknown until now because of complicated chemical reactions among many particle species into which they are decomposed in arc discharges.

This article describes a study to understand quantitatively physical properties of ammonia or mixture of nitrogen and hydrogen plasmas in a 10-kW-class direct-current arcjet. Spectroscopic measurement is carried out, and several plasma properties are examined from the data. Atomic electronic excitation and molecular rotational excitation temperatures are determined, and electron number densities are also estimated using Stark broadening of the hydrogen H β line. Their radial profiles are determined using Abel transformations.

Experimental Apparatus

Figure 1 shows the cross section of the 10-kW-class direct-current arcjet used for this study. The electrodes are water-cooled. A constrictor has a diameter of 6 mm and a length of 7 mm. A divergent nozzle has an exit diameter of 34 mm and an angle of 52°. The ratio of the cross-sectional area of the nozzle exit to that of the constrictor is 32.1. As shown in Fig.1(b), the anode is provided with quartz glass rings for arc observation and optical diagnostics. A cylindrical cathode made of 2% thoriated tungsten has a diameter of 10 mm. The gap between the electrodes, which is defined as the axial distance between the cathode tip and the constrictor upstream exit, is set to 2 mm. Ammonia and a mixture of nitrogen and hydrogen are used as propellants. The gas is injected tangentially from the upstream end of the discharge chamber. The input power in the gas is evaluated by measuring temperatures of cooling water through the electrodes and calculating the powers consumed into the electrodes. The thermal efficiency, which is defined as the ratio of the net input power into the gas to the total electrical input power, is estimated.

The arcjet is operated with input power levels of 3-12 kW at discharge currents of 70-150 A using a power supply with a current ripple up to 30% at 60 Hz. Time average values are measured in the present experiments. High-frequency discharge of 3 MHz and amplitude 2 kV is used for arc initiation. The arcjet is set on a flange of a vacuum tank, into which the heated gas is exhausted, as shown in Fig.2. The vacuum tank 0.8 m in diameter and 1.5 m long is evacuated with a mechanical booster 6000 m^3/h connected in series with a rotary pump 600 m^3/h.

---

* Associate Professor, Member JSASS/AIAA
** Graduate Student of Osaka University
+ Research Associate, Member JSASS
++ Professor, Member JSASS/AIAA

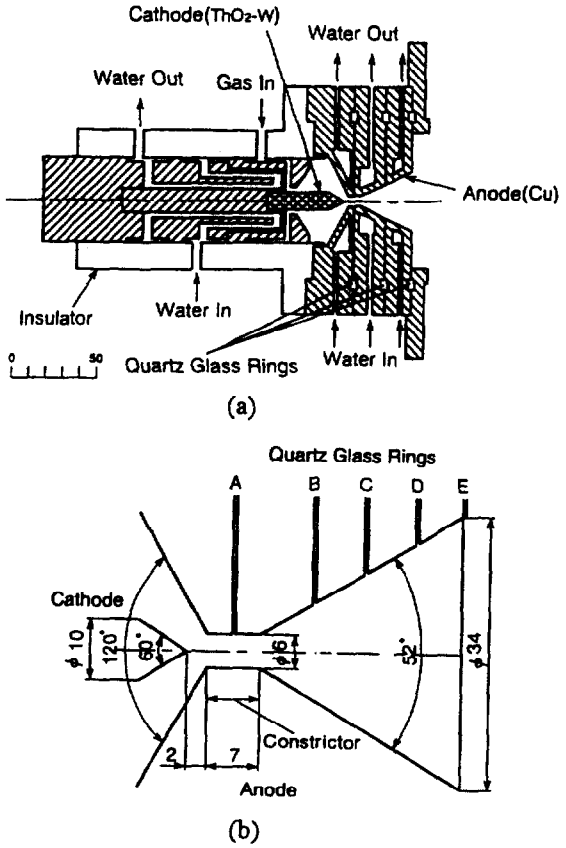

Fig.1 Cross section of 10-kW-class water-cooled direct-current arcjet. The expansion nozzle is exchanged to another one with quartz glass rings in different axial positions for optical measurement. (a) Configuration of arcjet. (b) Arrangement of electrodes and quartz glass rings.

Emission spectroscopic measurement is conducted as reliable plasma diagnostics in arcjet chambers. Light comes from the plasma through a quartz glass slit 0.5 mm in width, as shown in Fig.1(b). The emission is collected by a lens of 80 mm in focal length and is introduced into a 0.5-m monochrometer through an optical fiber. The monochrometer of diffraction-grating-type HAMAMATSU C5095 is provided with 150 and 2400 grooves/mm grating plates and a 1024-channel diode array detector, achieving spectral resolutions of 0.8 and 0.05 nm, respectively, per detector channel. Electron number densities and several plasma temperatures of electronic excitation for H and molecular rotational excitation for N_2 and NH are determined using the spectral data.[5,7] The electron number density is estimated from the Stark width of the hydrogen H β line 486.1 nm.

The spectral intensities measured in this experiment are line-of-sight values, measured by looking through the arc from the side perpendicular to the center line of the arcjet. For line-of-sight measurements, the intensity values correspond to integrated values of intensity as a function of position. The radially dependent emission coefficient is determined from the measured spectral intensities using well-known Abel transformations.[7] When axisymmetry of the emission was checked by rotating the electrodes, small deviations were observed

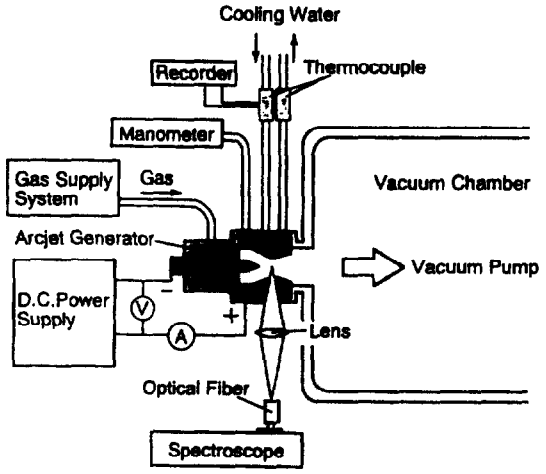

Fig.2 Experimental system of arcjet fixed on flange of vacuum tank.

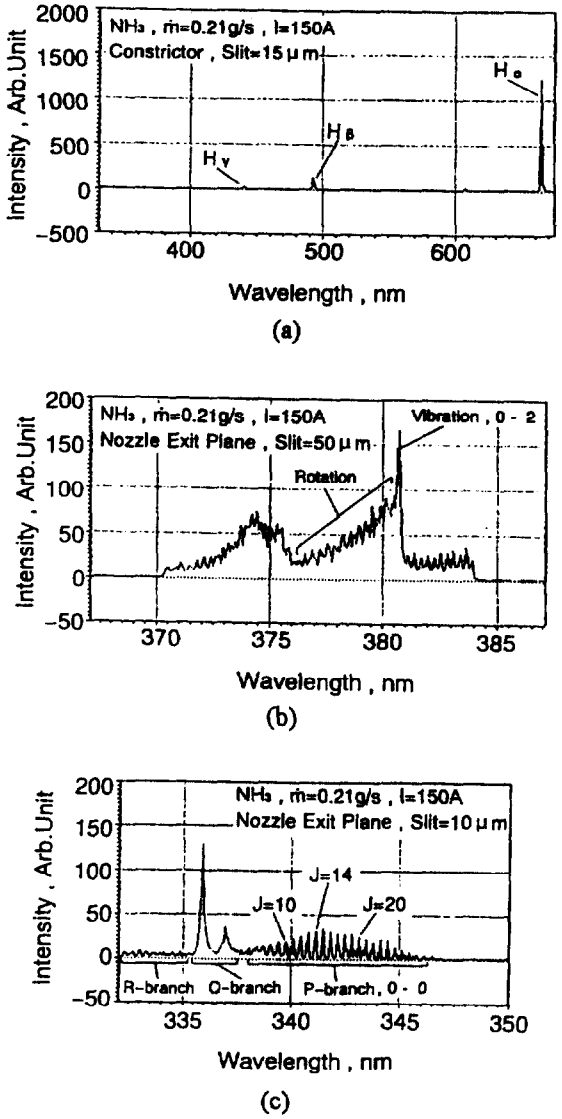

Fig.3 Typical spectra emitted from plasma in arcjet discharge chamber. (a) HI Balmer lines. (b) N_2 second positive bands. (c) NH bands.

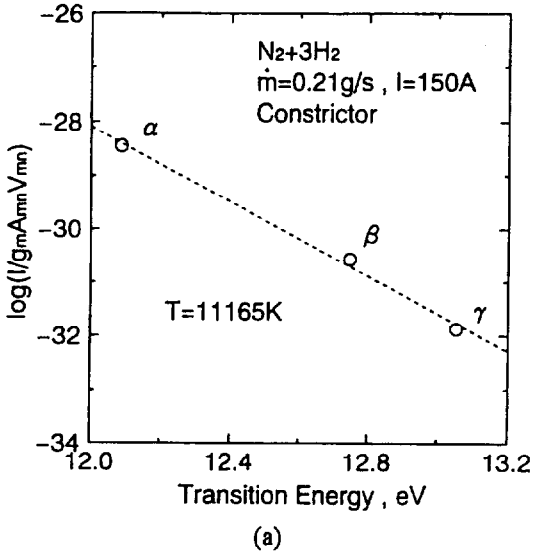

(a)

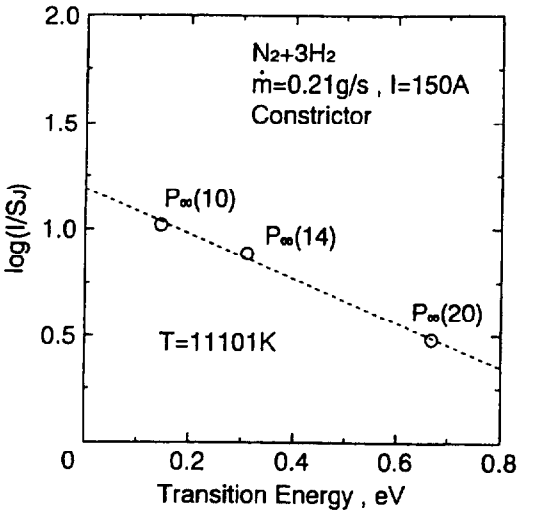

(b)

Fig.4 Typical Boltzmann plottings for determination of H-atom excitation temperature with HI Balmer lines and for determination of NH rotational temperature with P branch (0-0). The emission intensity is represented with the symbol I. (a) For determination of H-atom excitation temperature: the emission frequency is ν_{mn}, in which the subsymbol mn represents the transition from m to n energy level, the statistical weight of m energy level g_m and the atomic transition probability A_{mn}. (b) For determination of NH rotational temperature: the line strength factor is S_j.

owing to slight nonaxisymmetry of electrode arrangement and of arc attachment on the electrodes. As a result, an approximate axisymmetric profile of an average spectral intensity profile of five measurements is used. Also, the horizontally average spectral intensities are measured with a perpendicular interval of 0.25 mm.

The H-atom electronic excitation temperature is determined using a relative intensity method of spectral lines, i.e., by means of Boltzmann plotting with HI Balmer lines of 434.0, 486.1 and 656.3 nm, as shown in Figs.3(a) and 4(a), under the assumption of local thermodynamical equilibrium (LTE), in which the linearity of the Boltzmann plotting and the theoretical limiting criteria on electron density and local pressure were considered for estimation of separation from LTE.[5,8] The H-atom excitation temperature is considered to almost equal the temperature of free electrons in plasmas under LTE conditions. The relative intensity method can not be used to determine the rotational temperature of N_2 because the rotational lines are too close together and overlapped, as shown in Fig.3(b). Therefore, in general, the theoretical intensity distribution for a band is calculated with an assumed rotational temperature and compared to the measured spectrum.[9,10] The transition band of N_2 $C^3\Pi_u$-$B^3\Pi_g$ at 380.4 nm (second positive band) is used.[11,12] Since the emission for the first negative band of N_2^+ was very small even using an image intensifier, we could not evaluate the N_2^+ rotational temperatures.[5,7] In order to simply calculate radial profiles of rotational temperatures in the present study, after Abel transformations of measured emission intensities at 380.0 and 379.0 nm in the second positive band, the ratio of their two intensities at a same radial position is compared to a theoretical intensity ratio with an assumed rotational temperature. As shown in Fig.3(c), NH bands of electronic excitation $A_3\Pi$-$X_3\Sigma^-$, vibrational excitations (0-0) and (1-1) are intensively observed.[13,14] The rotational temperature for the P branch band (0-0) is calculated using the relative intensity method with Boltzmann plotting of $P_{00}(10)$, $P_{00}(14)$ and $P_{00}(20)$ at 339.6, 341.0 and 343.1 nm, respectively, as shown in Fig.4(b).[14,15]

Results and Discussion

Discharge Voltage and Vacuum Chamber Pressure

Figure 5 shows the discharge voltage vs. discharge current characteristics for ammonia and a mixture of N_2+nH_2, in which input powers of 5 and 10 kW are represented with the dashed lines. In Fig.5(b), the H_2 mole fraction n is varied from 0.5 to 3.0 at a total mass flow rate of 0.21 g/s, in which a H_2 mole fraction of 3.0 corresponds to that of ammonia. The discharge voltage gradually decreases with increasing discharge current at a constant mass flow rate for ammonia. This agrees with that for N_2+nH_2 at a constant of n. An increase in NH_3 mass flow rate also raises the voltage with a constant current. As shown in Fig.5(b), the discharge voltage increases with H_2 mole fraction because of an increase in total particle number. The discharge voltage for a mixture of N_2+3H_2 at n=3, corresponding to the mole fraction of NH_3, is higher than that for NH_3. This cause is considered as follows. Heat transfer due to molecules or atoms of hydrogen in N_2+3H_2 arcs is expected to be more efficient than that due to fragmental particles such as H, H_2, NH and NH_2 in NH_3 arcs. As a result, thermal pinch for the mixture of N_2+3H_2 is enhanced compared with that for NH_3, and the electric field for N_2+3H_2 is higher than that for NH_3.[5,7] Accordingly, the electrical input powers range from 4 to 12 kW for both ammonia and a mixture of nitrogen and hydrogen. The thermal efficiencies were 50-70 % for all operations. Figure 6 shows the dependence of input power and H_2 mole fraction on the pressure in the vacuum tank. The vacuum tank pressure increases linearly with input power at a

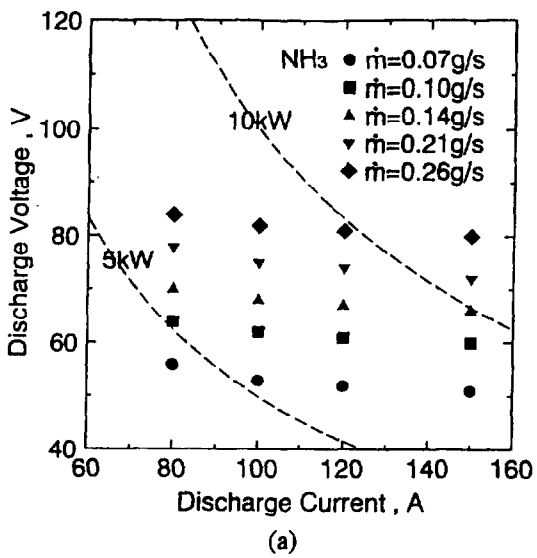

Fig.5 Discharge voltage vs. discharge current characteristics of direct-current arcjet. Input powers of 5 and 10 kW are represented with the dashed lines. (a) Ammonia. (b) Mixture of nitrogen and hydrogen: the H_2 mole fraction n is varied from 0.5 to 3.0, and the H_2 mole fraction of 3.0 corresponds to that of ammonia.

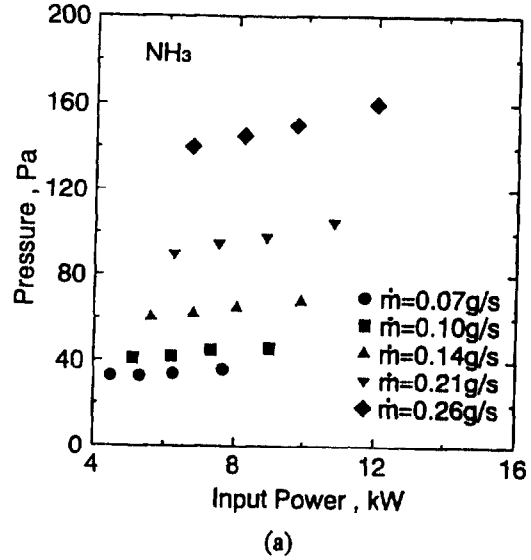

Fig.6 Vacuum tank pressure vs. input power characteristics of direct-current arcjet. (a) Ammonia. (b) Pressure vs. H_2 mole fraction characteristics for mixture of nitrogen and hydrogen.

constant mass flow rate for ammonia. Since this behavior is mainly due to a linear increase in total particle flux, dissociation of ammonia is found to be enhanced by increasing input power. As shown in Fig.6(b), an increase in H_2 mole fraction also raises linearly the pressure in the vacuum tank. The pressure for the mixture of N_2+3H_2 is slightly higher than that for NH_3. This is expected because the flux of H_2 and H in N_2+3H_2 discharges is higher than that of fragmental particles in NH_3 discharges. The pressures range from 20 to 160 Pa in the present experiments.

Arc Plasma in Constrictor

Figures 7 and 8 show the radial profiles of H-atom excitation temperature and electron number density, respectively, in the constrictor. The input power for N_2+3H_2 is slightly higher than that for NH_3 at a constant mass flow rate because of the higher discharge voltage for N_2+3H_2 than that for NH_3, as shown in Fig.5(b). The H-atom excitation temperatures for both gases have maxima of 8000-12000 K on the center axis of the arcjet, and they decrease radially outward up to about 6000 K at 1.75 mm in radius, although their profiles are almost flat within about 0.25 mm in radius. The characteristics of the electron number densities shown in Fig.8 also agree with those of the temperatures. An increase in mass flow rate raises the maxima on the center line of the arcjet. The temperature for N_2+3H_2 is higher than that for NH_3 at the center axis with the large mass flow rate of 0.21 g/s because of enhanced thermal pinch, although the temperature with the low mass flow rate of 0.10 g/s and the electron number densities do not change significantly for N_2+3H_2 and NH_3.[5,7] This characteristic agrees with the discharge voltage vs. current characteristics as shown in Fig.5(b). Also, the maximum temperature on the axis increased linearly with input power, and the characteristic

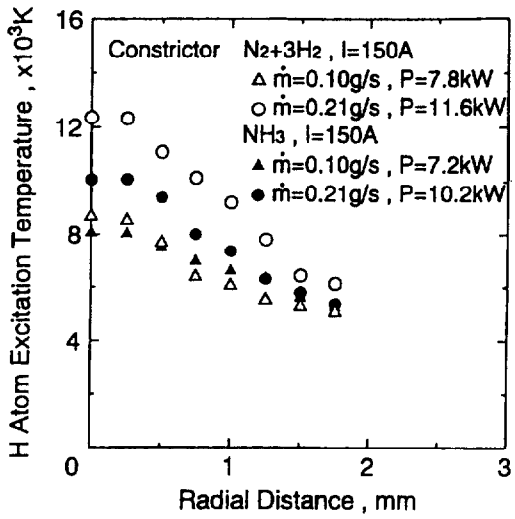

Fig.7 Radial profiles of H-atom excitation temperature in constrictor.

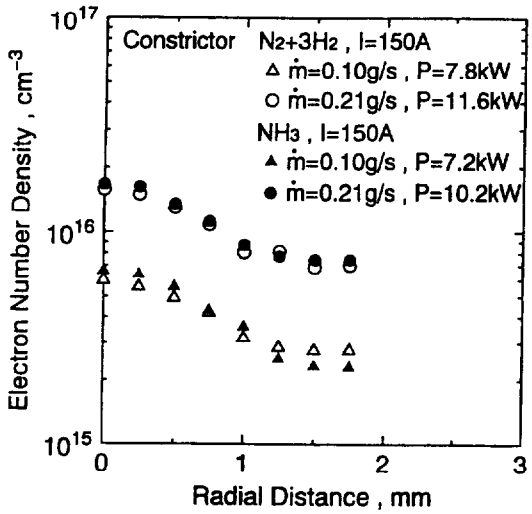

Fig.8 Radial profiles of electron number density in constrictor.

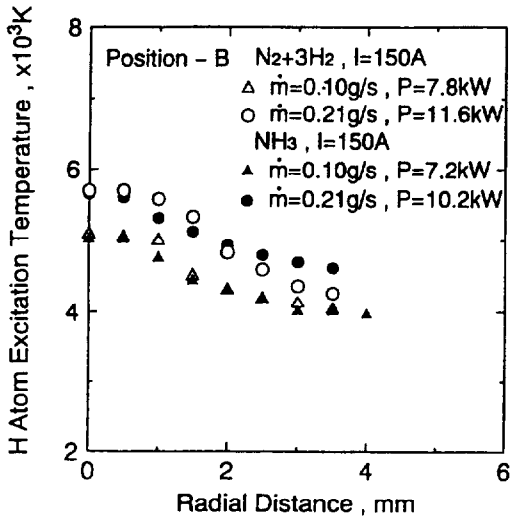

Fig.9 Radial profiles of H-atom excitation temperature at axial position B in expansion nozzle.

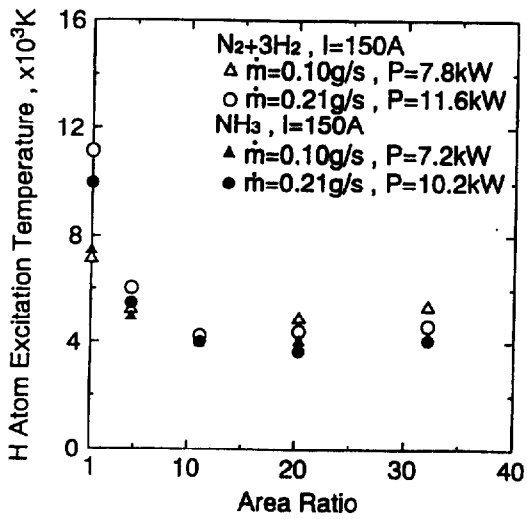

Fig.10 Axial variations of H-atom excitation temperature in expansion nozzle. The area ratio is defined as the ratio of the axial-plane cross-sectional area of the expansion nozzle to that of the constrictor.

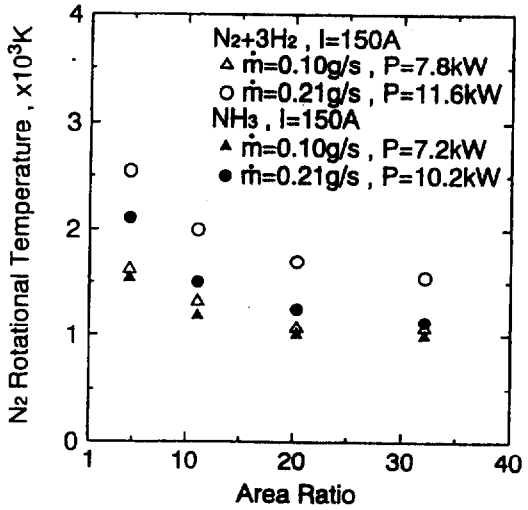

Fig.11 Axial variations of N_2 rotational temperature in expansion nozzle. The area ratio is defined as the ratio of the axial-plane cross-sectional area of the expansion nozzle to that of the constrictor.

line was independent of mass flow rate under these operational conditions.

Nonequilibrium Plasmas in Expansion Nozzle

Figure 9 shows the radial profiles of H-atom excitation temperature at the axial position B in the expansion nozzle. The temperature on the center axis of the arcjet decreases downstream from 8000-12000 K in the constrictor, as shown in Fig.7, to 5000-6000 K at the position B. The temperature at the position B gradually decreases radially outward compared with that in the constrictor. Therefore, plasma is found to be expanded radially and axially. Also, the H-atom excitation temperature for N_2+3H_2 almost equals that for NH_3. It is noted that we could not evaluate H-atom excitation temperatures at axial positions downstream from the

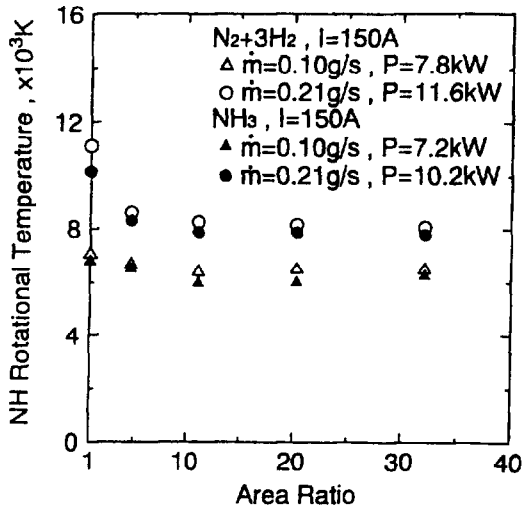

Fig.12 Axial variations of NH rotational temperature in expansion nozzle. The area ratio is defined as the ratio of the axial-plane cross-sectional area of the expansion nozzle to that of the constrictor.

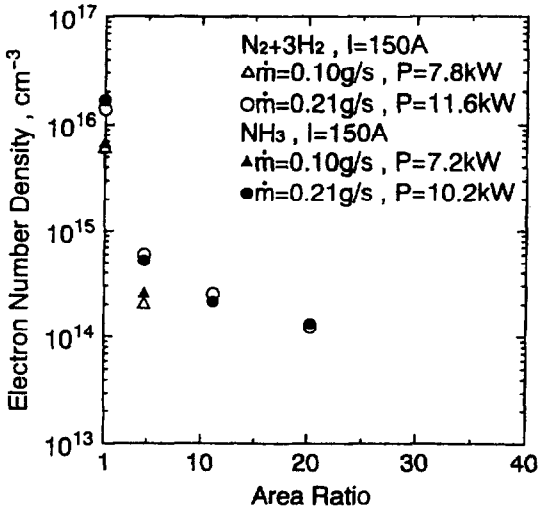

Fig.13 Axial variations of electron number density in expansion nozzle. The area ratio is defined as the ratio of the axial-plane cross-sectional area of the expansion nozzle to that of the constrictor.

position B because of large experimental errors.

Figures 10-12 show the axial variations of excitation temperatures of H atom, N_2 rotation and NH rotation, respectively, in the expansion nozzle. These values are estimated from horizontally average spectral intensities in the present line-of-sight measurements. The N_2 rotational temperature in the constrictor could not be evaluated because of noisy experimental data. The H-atom excitation temperature drastically decreases from 7000-11000 K at the downstream exit of the constrictor to about 4000 K at an area ratio of about 10, and then it is kept constant downstream. The N_2 rotational temperature also decreases downstream up to 1000-1500 K. On the other hand, the NH rotational temperature does not axially decrease significantly. It is almost constant through the nozzle. The NH rotational temperature on the center axis ranges from 7000 to 11000 K. Since the H-atom excitation temperature on the center axis almost equals the NH rotational temperature, the plasma in the constrictor is expected to be nearly in temperature equilibrium. However, in the expansion nozzle the plasma is in thermodynamical nonequilibrium. In general, N_2 rotational temperatures decrease downstream through the nozzle, as shown in Fig.11, owing to the strong coupling between the translational temperatures and them.[4,5,7] This behavior does not agree with that for the NH rotational temperature. The cause is explained as follows.[16-18] Polar molecules such as CH and NH have longer relaxation times of rotational excitation than those of molecules without polars. Since the times are beyond the characteristic flow time on the order of 10^{-6} s in the nozzle, the NH rotational temperature is almost kept a constant of that in the constrictor. However, since chemical luminescence, whose physical mechanism is unknown clearly, occurs in the polar molecules, an intensive NH band emission is observed even in the low-pressure expansion nozzle with few deexcitation collisions. As shown in Fig.13, the electron number density also axially decreases on the order from 10^{16} cm^{-3} in the constrictor to 10^{14} cm^{-3} at an area ratio of 5-20. We could not evaluate the electron density below 10^{14} cm^{-3} on account of a narrow width of the Hβ line spectrum. As a result, plasma is expected to be extremely expanded axially and radially in the supersonic nozzle.

Conclusions

Spectroscopic measurement was conducted to understand the arc structure and the flowfield in a 10-kW-class water-cooled direct-current arcjet. Ammonia and a mixture of nitrogen and hydrogen were used as propellants. In the mixture of N_2+nH_2, the H_2 mole fraction n was varied from 0.5 to 3.0, in which a mole fraction of 3.0 corresponded to that of ammonia. The discharge voltage and the vacuum tank pressure for N_2+3H_2 were higher than those for NH_3 at a constant discharge current and a constant input power, respectively, because of the difference of particles species generated in their arc discharges. These characteristics agreed with those of H-atom excitation temperatures and electron number densities in the constrictor. The NH_3 and N_2+3H_2 plasmas in the constrictor were expected to be nearly in a temperature-equilibrium condition. On the other hand, the plasmas in the expansion nozzle were in thermodynamical nonequilibrium, because the electron number densities drastically decreased downstream. As a result, the H-atom electronic excitation temperature and the N_2 rotational excitation temperature decreased from 7000-11000 K in the constrictor to about 4000 K and to 1000-1500 K, respectively, on the nozzle exit at input powers of 7-12 kW. However, the NH rotational excitation temperature did not axially decrease significantly because of its longer relaxation time of rotational excitation, although an intensive NH band emission was observed even in the low-pressure expansion nozzle with few deexcitation collisions owing to chemical luminescence.

References

1. Tahara, H., Sakakibara, T., Onoe, K. and Yoshikawa, T.," Discharge Characteristics and Inner Plasma Feature of a High Power DC Arcjet Thruster," AIAA Paper 90-2534, 1990.
2. Tahara, H., Sakakibara, T., Onoe, K. and Yoshikawa, T.," Experimental and Numerical Studies of a 10 kW Water-Cooled Arcjet Thruster," Proc. AIDAA/AIAA/DGLR/JSASS 22nd Int. Electric Propulsion Conf., Vol.1, Paper No. 91-015, 1991.
3. Tahara, H., Uda, N., Onoe, K., Tsubakishita, Y. and Yoshikawa, T.," Optical Measurement and Numerical Analysis of Medium-Power Arcjet Non-Equilibrium Flowfields," AIAA/AIDAA/DGLR/JSASS 23rd Int. Electric Propulsion Conf., Paper No. 93-133, 1993.
4. Uda, N., Tahara, H., Onoe, K. and Yoshikawa, T.," Flowfield Analysis of an Arcjet Thruster," Proc. 18th Int. Symp. Space Technology and Science, Vol.1, 1992, pp.277-285.
5. Tahara, H., Uda, N., Onoe, K., Tsubakishita, Y. and Yoshikawa, T.," Discharge Features in a Steady-State Nitrogen Arcjet Engine with an Expansion Nozzle," IEEE Trans. Plasma Science, Vol.22, 1994, pp.58-64.
6. Komiko, K., Zhang, L., Onoe, K., Tahara, H. and Yoshikawa, T.," Optical Measurement and Numerical Analysis of 10-kW-Class Steady-State Arcjet Flowfields," 19th Int. Symp. Space Technology and Science, Paper No. 94-a-51, 1994.
7. Tahara, H., Komiko, K., Yonezawa, T., Andoh, Y. and Yoshikawa, T.," Thermodynamical Nonequilibrium Nitrogen Plasmas in a Direct-Current Arcjet Engine Nozzle," IEEE Trans. Plasma Science, Vol.24, 1996, pp.218-225.
8. Wiese, W.L., Smith, M.W. and Glennon, B.M., Atomic Transition Probabilities, U.S.GPO, Washington, 1963.
9. Herzberg, G., Molecular Spectra and Molecular Structure, I. Spectra of Diatomic Molecules, New York, van Nostrand, 1959.
10. Phillips, D.M.," Determination of Gas Temperature from Unresolved Bands in the Spectrum from a Nitrogen Discharge," J. Phys. D: Appl. Phys., Vol.8, 1975, pp.507-521.
11. Nicholls, R.W.," Frank-Condon Factors to High Vibrational Quantum Numbers I: N_2 and N_2^+," J. Research of the National Bureau of Standards - A. Physics and Chemistry -, Vol.65A, 1961, pp.451-460.
12. Pearse, R.W.B. and Gaydon, A.G., The Identification of Molecular Spectra, 2nd Ed. New York, Wiley, 1950.
13. Crofton, M.W., Welle, R.P., Janson, S.W. and Cohen, R.B.," Temperature, Velocity and Density Studies in the 1kW Ammonia Arcjet Plume by LIF," AIAA Paper 92-3242, 1992.
14. Lents, J.M.," An Evaluation of Molecular Constants and the Transition Probabilities for the NH Free Radical," J. Quantitative Spectroscopy and Radiative Transfer, Vol.13, 1973, p.297.
15. Brazier, C.R., Ram, R.S. and Bernath, P.F.," Fourier Transform Spectroscopy of the $A^3\Pi$-$X^3\Sigma^-$ Transition of NH," J. Molecular Spectroscopy, Vol.120, 1986, pp.381-402.
16. Raiche, G.A. and Jeffries, J.B.," Laser-Induced Fluorescence Temperature Measurements in a DC Arcjet Used for Diamond Deposition," Appl. Opt., Vol.32, 1993, pp.4629-4635.
17. Reeve, S.W. and Weimer, W.A.," Plasma Diagnostics of a Direct-Current Arcjet Diamond Reactor. II. Optical Emission Spectroscopy," J. Vac. Sci. Technol., Vol.A13, 1995, pp.359-367.
18. Gaydon, A.G. and Wolfhard, H.G., Flames, Their Structure, Radiation and Temperature, 4th ed. New York, Wiley, 1979.